

UC San Diego

UC San Diego Previously Published Works

Title

Destructin-1 is a collagen-degrading endopeptidase secreted by *Pseudogymnoascus destructans*, the causative agent of white-nose syndrome

Permalink

<https://escholarship.org/uc/item/2986z4qj>

Journal

Proceedings of the National Academy of Sciences of the United States of America, 112(24)

ISSN

0027-8424

Authors

O'Donoghue, Anthony J
Knudsen, Giselle M
Beekman, Chapman
[et al.](#)

Publication Date

2015-06-16

DOI

10.1073/pnas.1507082112

Peer reviewed

1
2
3
4
5
6
7
8
9
10
11
12
13
14
15
16
17
18
19

**Destructin-1 is a Collagen-Degrading Endopeptidase Secreted by
P. destructans, the Causative Agent of White-Nose Syndrome**

Running Title: Collagen-Degrading Peptidase Destructin-1

Anthony J. O’Donoghue^{1#}, Giselle M. Knudsen^{1#}, Chapman Beekman²,
Jenna Perry², Alexander D. Johnson³, Joseph L. DeRisi³, Charles S. Craik¹,
and Richard J. Bennett^{2*}

¹Department of Pharmaceutical Chemistry, University of California San Francisco (UCSF),
San Francisco, California, United States of America.

³Department of Biochemistry and Biophysics, University of California San Francisco (UCSF),
San Francisco, California, United States of America, and the Howard Hughes Medical Institute,
San Francisco, CA.

²Brown University, 171 Meeting St, Providence, RI 02912.

#These authors contributed equally to the work

*To whom correspondence should be addressed. E-mail: richard_bennett@brown.edu

20 **Abstract**

21 *P. destructans* is the causative agent of White-Nose Syndrome (WNS), a devastating
22 disease that has caused the deaths of millions of bats in North America. This psychrophilic
23 fungus targets hibernating bats, resulting in their premature arousal from stupor with
24 catastrophic consequences. Despite the impact of WNS, little is known about the fungus or how
25 it mediates infection of the mammalian host. *P. destructans* is not amenable to genetic
26 manipulation, and therefore understanding the proteins involved in infection requires
27 alternative approaches. Here, we identify a set of proteolytic enzymes that are a part of a broad
28 arsenal of hydrolytic enzymes secreted by *P. destructans*. Collagen, the major structural protein
29 in mammals, was degraded by secreted peptidases from this fungus, and we therefore used a
30 novel and unbiased substrate profiling technique to define active peptidases in the *P. destructans*
31 secretome. These experiments revealed that endopeptidases are the major proteolytic activities
32 secreted by *P. destructans*. A serine endopeptidase, hereby-named Destructin-1, was
33 subsequently identified, and a recombinant form overexpressed and purified. Biochemical
34 analysis of Destructin-1 showed that it mediated collagen degradation, and a potent inhibitor of
35 peptidase activity was identified. Treatment of *P. destructans* conditioned media with this
36 antagonist blocked collagen degradation and facilitated the detection of additional secreted
37 proteolytic activities, including aminopeptidases and carboxypeptidases. These results provide
38 the first molecular insights into the secretome of *P. destructans*, and identify serine
39 endopeptidase(s) that have the clear potential to facilitate tissue invasion and pathogenesis in
40 the mammalian host.

41

42

43 **Significance Statement**

44 This work is the first to identify molecular factors produced by the fungus *P. destructans*,
45 the causative agent of White-Nose Syndrome in bats. Our study reveals the repertoire of redox
46 enzymes and hydrolytic enzymes secreted by *P. destructans*. We establish that a secreted serine
47 peptidase, Destructin-1, is a major component of the *P. destructans* secretome. This peptidase
48 was purified and shown to degrade collagen, the major structural protein in mammalian
49 connective tissue. Furthermore, chemical inhibition of Destructin-1 blocked collagen
50 degradation in conditioned media from *P. destructans*. We therefore propose that serine
51 endopeptidase(s) aid in invasive growth and tissue destruction by the fungus, and represent
52 potential targets for therapeutic intervention in WNS.

53 \body

54 Introduction

55 White-Nose Syndrome (WNS) has caused the deaths of more than 6 million bats in North
56 America since its discovery in a New York cave in 2006 (1, 2). It has spread to 22 US states and
57 5 Canadian provinces, with nearly 100% mortality observed in some locations (3). This
58 represents one of the most precipitous declines in North American wildlife seen in the past
59 century (1). If current trends continue, 25 species of hibernating bats in the US will be
60 threatened, with some previously common species becoming extinct (4). In addition to the
61 devastating impact on bat populations, the disease is an economical threat to the North American
62 agricultural industry, where the loss of bats could cost the industry more than 3 billion dollars a
63 year (5).

64 The causative agent of WNS is the fungus *Pseudogymnoascus destructans* (formerly
65 *Geomyces destructans*) (6), which grows as a white layer on the muzzle, wings and ears of bats
66 (7). *P. destructans* is a psychrophilic fungus that belongs to the family *Pseudeurotiaceae*, and
67 appears to be an invasive species with no close relatives in the hibernacula of North America (6).
68 *P. destructans* targets hibernating bats whose immune function is reduced and whose body
69 temperatures are lowered. The fungus grows optimally at these lower temperatures, with
70 maximal growth between 12°C and 16°C (8). The injuries associated with fungal infections
71 result in increased arousal in hibernating bats and the premature use of fat storage, with the
72 outcome that bats are emaciated and die before the end of hibernation. Infection involves deep
73 penetration of the subcutaneous tissue by fungal hyphae, causing ulcerative necrosis and tissue
74 destruction (7, 9-11). *P. destructans* typically forms more superficial infections in European bat
75 populations, with no evidence for associated mortality (9, 12), although a recent study also found
76 evidence of invasive WNS lesions in European bats (13). Current models suggest that *P.*

77 *destructans* is an invasive species that originated in Europe, where native bat species may be
78 more resistant to the most debilitating forms of the disease (9).

79 There is currently little information as to the mechanism by which *P. destructans* causes
80 tissue invasion or infection in bats. To begin to address the properties of *P. destructans*
81 associated with WNS, we focused on secreted enzymes produced by this fungus. Many fungal
82 pathogens secrete a number of important enzymes that promote pathogenesis, of which
83 proteolytic activities have been the most intensively studied (14, 15). Peptidases play diverse
84 roles in fungal disease as illustrated by the SAP family of aspartyl peptidases produced by
85 pathogenic *Candida* species. In *Candida albicans*, the most common human fungal pathogen,
86 these enzymes are implicated in multiple processes including adhesion to epithelial cells,
87 degradation of host proteins, survival and escape from immune cells, and invasion of mucosal
88 tissues (16). Aspartyl and serine peptidases are also associated with dermatophytes that infect
89 the *stratum corneum*, nails, and hair of animals. Here, they are implicated in promoting
90 adherence to host cells and keratin degradation during tissue invasion (17, 18). Both *Candida*
91 species and dermatophytes display expanded protein families of peptidases, supporting the
92 contention that these factors are key virulence factors (15, 18). Given their central role in
93 pathogenesis, there is also now considerable interest in identifying inhibitors of fungal
94 peptidases as potential therapeutic drugs (19). Other virulence factors secreted by mammalian
95 fungal pathogens include lipolytic enzymes (lipases and phospholipases) that can further
96 mediate the destruction of epithelial tissues (20).

97 In this work, we analyzed the secretome of *P. destructans* and found that most proteins
98 are predicted to have hydrolytic activity, including a number of peptidases, lipases and
99 glycosidases, or are redox enzymes such as catalase peroxidase. Secreted peptidases included
100 those with the ability to degrade collagen, the major component of mammalian connective tissue.
101 To address global proteolytic activity, an unbiased substrate profiling assay was performed, and

102 revealed that endopeptidases are the major proteolytic activities secreted by *P. destructans*.
103 Using conventional chromatography and an internally quenched fluorescence reporter substrate,
104 the major endopeptidase activity was isolated and shown to be associated with a serine
105 endopeptidase, hereby named Destructin-1. Recombinant Destructin-1 was overexpressed and
106 purified, and shown to actively degrade collagen. Significantly, Destructin-1 activity was
107 potently blocked by the serine peptidase inhibitor chymostatin, and treatment of conditioned
108 media with this inhibitor blocked collagen degradation. Destructin-1 therefore represents a
109 novel virulence factor for *P. destructans*, with the ability to promote tissue damage and invasion
110 in the mammalian host.

111

112

113 **Results**

114 **Hydrolytic enzymes are the major proteins secreted by *P. destructans***

115 In order to identify proteins secreted by *P. destructans*, fungal cells were grown in RPMI
116 medium at 13°C for 7 days. Proteins from the conditioned medium were analyzed by peptide
117 sequencing using liquid chromatography-tandem mass spectrometry (LC-MS/MS), and targets
118 searched against the *P. destructans* genome. In total, 44 proteins were identified in the
119 secretome, of which 33 were found in at least 2 of 3 independent experiments (Tables S1-S3).
120 Many of these proteins were predicted to have enzymatic activity based on sequence analysis
121 and were broadly grouped as hydrolytic enzymes, glycosyl transferases, or redox enzymes. The
122 hydrolytic enzymes included 13 glycosidases, 6 peptidases, 2 lipases and 1 amidase (Fig. 1A).
123 The diversity of hydrolytic enzymes present is consistent with previous reports of multiple
124 hydrolytic activities in *P. destructans* cultures, although the proteins responsible for these
125 activities were not determined (21, 22). Many of these enzymes are likely to play a role in

126 supporting saprophytic growth, but fungal peptidases can also function in supporting host-
127 pathogen interactions (14, 15).

128 The *P. destructans* secretome included three serine endopeptidases, two serine
129 carboxypeptidases, and an aspartyl endopeptidase (Fig. 1B). The aspartyl endopeptidase shared
130 21% to 26% sequence identity with the *C. albicans* Sap protein family (23). The two
131 carboxypeptidases were GMDG_06096, which is closely related to carboxypeptidase Y from
132 *Saccharomyces cerevisiae* (56% sequence identity), and GMDG_05452, which is similar to
133 carboxypeptidase II from *Aspergillus niger* (58% sequence identity). The three serine
134 endopeptidases exhibited similarity to cuticle-degrading enzymes secreted by entomopathogenic
135 fungi (24). These included GMDG_06417 and GMDG_08491, which share 90% amino acid
136 identity and are hereby named Destructin-1 and Destructin-2, respectively. A third serine
137 peptidase, GMDG_04447, showed 56% identity to Destructin-1 and was named Destructin-3 (Fig.
138 S1).

139

140 **Collagen and synthetic peptides are degraded by secreted peptidases**

141 One of the primary sites of infection by *P. destructans* is the membranous skin of bats'
142 wings, where it causes extensive invasion and tissue damage (25). To test whether peptidases in
143 the secretome could contribute to wing damage and tissue invasion, conditioned media was
144 incubated with azo dye-impregnated collagen. We observed a time-dependent release of dye
145 over a 54 hour time course (Fig. 2A). This finding led us to perform a comprehensive analysis of
146 the proteolytic activity secreted from *P. destructans* with the goal of identifying and
147 characterizing peptidase(s) responsible for collagen degradation. We used a global and unbiased
148 substrate profiling assay to uncover the secreted proteolytic signature of this fungus. This assay
149 consists of a mixture of 124 physiochemically diverse peptides that are each 14-residues in
150 length. Cleavage at any one of the 1612 peptide bonds within these peptides can be readily

151 detected by LC-MS/MS sequencing (Fig. 2B) (26). Co-incubation with the *P. destructans*
152 secretome resulted in 137 cleavage sites detected after 1-hour incubation and 308 cleavage
153 events after 20 hours incubation. The complexity of these hydrolytic events is illustrated in
154 three example peptides where multiple cleavage sites were often detected within each peptide
155 (Fig. 2C). Using iceLogo software (27), a substrate signature was generated corresponding to the
156 global specificity of the peptidases in the media. These peptidases exhibited a preference for
157 hydrophobic residues at P4, Ile and norleucine at P2, Gln, Phe and Trp at P1, and Ile at P2' (Fig.
158 2D). In addition, the detected peptidases showed a low tolerance for Glu in almost all positions
159 and Val, Pro and Gly at P1. Time-dependent trimming of amino acids from the termini of these
160 peptides was not evident, indicating that exopeptidase activity was rare and that the major
161 activity was due to one or more endopeptidases.

162

163 **Endopeptidase activity from *P. destructans* can be monitored with fluorescent substrates**

164 A diverse set of 15 internally quenched (IQ) fluorescent peptides (Table S5) was screened
165 to identify substrates that could be used to monitor endopeptidase activity in *P. destructans*
166 conditioned media. Two of the 15 peptides were efficiently cleaved (Fig. 3A) and the sites of
167 cleavage determined by MALDI-TOF mass spectrometry (Fig. S2). These substrates consisted of
168 tQAS↓SRS (IQ8) and PKRLSAL↓L (IQ12), where t represents tert butyl glycine and ↓ the
169 position of cleavage. Analysis of these cleavage sites revealed the presence of a hydrophobic
170 residue at P4 and Ala at P2 in both substrates, consistent with the global iceLogo substrate
171 signature (Fig. 2D). However, these initial experiments did not determine whether the
172 endopeptidase activity is derived from one or multiple enzymes.

173

174 **Purification and identification of endopeptidases from *P. destructans***

175 To isolate the peptidase(s) responsible for cleavage of IQ8 and IQ12 peptides, conditioned
176 *P. destructans* medium was applied to a DEAE sepharose column and eluted fractions assayed for
177 proteolytic activity (Fig. 3B). Fractions with activity were pooled, applied to a Phenyl sepharose
178 column, and eluted fractions assayed again using IQ8 and IQ12 (Fig. 3C). Proteolytic activity on
179 these substrates was found to co-purify, and active fractions pooled and subjected to gel
180 filtration chromatography. Activity from the gel filtration column identified a peptidase with a
181 molecular weight of ~25 kDa (Fig. 3D). Analysis of protein from the active fractions showed two
182 major bands on a silver-stained SDS-PAGE gel (Fig. 3D, inset). These bands were excised and
183 analyzed by LC-MS/MS, and the upper band shown to represent Destructin-1 (GMDG_06417).
184 The lower, minor band was GMDG_08104, a highly abundant protein in the secretome that
185 contains a WSC domain. A number of unique peptides support the specific identification of
186 Destructin-1 (Fig. S1 and Table S4); however, due to the high sequence conservation with
187 Destructin-2 it is not possible to exclude its presence at lower abundance. Indeed, analysis of
188 individual protein bands excised after SDS-PAGE analysis of the Phenyl sepharose eluate showed
189 the presence of Destructin-2-specific peptides (Table S4).

190 These results suggest that Destructin-1 encodes the major proteolytic activity responsible
191 for cleavage of both IQ8 and IQ12 substrates. This enzyme shares 50-52% amino acid identity
192 with secreted cuticle-degrading peptidases from nematode-trapping fungi such as *Dactylella*
193 *varietas* and *Arthrobotrys conoides* (DvS8 and AcAC1, Fig. S1) (28, 29). In addition, Destructin-1
194 shares 46% identity with EaS8 (Fig. S1), a broad-spectrum endopeptidase from *Engyodontium*
195 *album* that is stable in SDS, urea, chelating agents and sulfhydryl reagents, and is commercially
196 marketed as “Proteinase K”. These enzymes utilize a catalytic triad of aspartic acid, histidine,
197 and serine residues (30), which are conserved in Destructin-1 at positions 160, 192, and 345,
198 respectively (Fig. S1).

199 Destructin-1, -2, and -3 contain an *N*-terminal signal sequence and a pro-domain that are
200 predicted to be removed during secretion and catalytic maturation, respectively. Analysis of the
201 N-terminus of Destructin-1 using SignalP 4.0 (31) identified a signal peptide (residues 2-20), that
202 was highly conserved with Destructin-2 and Destructin-3 (Fig. S1). Protein alignment with other
203 fungal enzymes predicted auto-catalytic processing of the Destructin-1 pro-domain occurs after
204 Asn¹¹⁹ to yield a mature peptidase of 27.7 kDa, which correlates with its elution size from gel
205 filtration (Fig. 3D). Peptide sequencing showed coverage exclusively within the mature
206 peptidase domain (highlighted in Fig. S1) and the absence of tryptic peptides corresponding to
207 the pro-domain (Ala²¹-Asn¹¹⁹). This establishes that the protein species detected here is the
208 activated form.

209

210 **Expression and characterization of recombinant Destructin-1**

211 To further characterize the activity of Destructin-1, a recombinant form of the pro-
212 enzyme was expressed with a C-terminal hexahistidine tag and purified from *Pichia pastoris* (Fig.
213 S3A). The resulting major band on a SDS-PAGE gel was excised and analyzed by MS sequencing
214 and Edman degradation. These results established the identity of recombinant Destructin-1 and
215 confirmed that the pro-enzyme is auto-processed between Asn¹¹⁹ and Ala¹²⁰ (Fig. S1). The
216 recombinant Destructin-1 hydrolyzed IQ8 and IQ12 substrates with optimal activity between pH
217 9 and 10, and no activity was evident below pH 4.2 (Fig. S3B).

218

219 **Degradation of collagen by Destructin-1**

220 Destructin-1 was assayed with azo dye-impregnated collagen for 72 hours and shown to
221 release dye in a time-dependent manner (Fig. 4A). The recombinant enzyme was also incubated
222 with soluble rat-tail collagen and the hydrolytic products assessed by SDS-PAGE and coomassie
223 staining. As shown in Fig. 4B, collagen consists of several major protein bands; the lower

224 molecular weight α -bands at \sim 120 kDa consist only of triple helical protein while the higher
225 molecular weight β -bands contain additional non-helical regions. Destructin-1 rapidly degraded
226 the β -bands but did not cleave the alpha bands, even after extended incubation. These
227 experiments reveal that Destructin-1 readily degrades the non-helical regions of collagen that
228 function in the cross-linking of the helical components.

229

230 **Rational design of optimal fluorescent substrates for Destructin-1**

231 The substrate specificity of recombinant Destructin-1 was further investigated using an
232 expanded MSP-MS assay containing 228 tetradecapeptides. Using 10 nM of enzyme, 197 peptide
233 bonds were cleaved within 5 minutes, with a preference for Phe, Gln and Tyr at P1. Hydrophobic
234 residues were preferred at P4 and P2, with positively charged or bulky residues at P3. On the
235 prime side of the scissile bond Lys and Thr were preferred at P1' and Ile, Trp and Tyr at P2' (Fig.
236 4C).

237 The MSP-MS assay was validated as a tool for defining the substrate specificity of
238 recombinant PdSP1 by direct comparison with specificity data generated using a positional
239 scanning synthetic combinatorial library (PS-SCL). The PS-SCL assay has been used to profile the
240 P1 to P4 substrate specificity of more than 90 endopeptidases, most of which are serine and
241 cysteine peptidases (32). This assay consists of 80 sub-libraries each containing 8,000 unique
242 tetrapeptides linked to a fluorogenic 7-amino-4-carbamoylmethylcoumarin group on the C-
243 terminus. This assay cannot be used to characterize complex protease mixtures such as
244 conditioned media due to an inability to detect aminopeptidase and carboxypeptidases activity
245 and a requirement for >5 μ g of each peptidase. As was observed in the MSP-MS assay, PdSP1
246 preferentially cleaved substrates containing hydrophobic residues at P4, positively charged
247 residues at P3, small or flexible residues at P2, and large, bulky residues at P1 (Fig. 4E). Both
248 assays showed a strong positive correlation of 0.86, 0.93, 0.54 and 0.73 (Pearson chi-squared

249 test) at positions P4, P3, P3 and P1, respectively (Table S6). This substrate signature represents
250 the most detailed specificity profile of a peptidase from a fungal species to date.

251 Based on the substrate specificity data, we predicted that IQ8 and IQ12 were suboptimal
252 substrates for Destructin-1. We have previously synthesized improved substrates for peptidases
253 based on the auto-activation site of the enzyme (33) or on the optimal sequences found in the
254 substrate specificity profile (34). An IQ substrate was therefore synthesized corresponding to
255 the P4 to P4' residues at the pro-Destructin-1 auto-activation site (VQAN-SLET) with flanking
256 methylcoumarin and dinitrophenol groups (IQ-Pro). An additional IQ substrate was synthesized
257 corresponding to the preferred residues in the P4 to P4' positions from the MSP-MS assay (IQ-
258 Opt). IQ-Opt was the most efficiently cleaved substrate with a k_{cat}/K_m of $14.3 \times 10^6 \text{ M}^{-1} \text{ s}^{-1}$,
259 which is a 10-fold improvement over IQ8 and 6-fold more efficient than IQ-Pro (Fig. 4D). Both
260 IQ-Pro and IQ-Opt could be accommodated into a homology model for the destructin-1 structure
261 (Fig. 4F and Fig. S4). In the homology model, P3' and P4' positions of the peptide do not
262 significantly interact with the enzyme, but there are deep hydrophobic S1 and S2 pockets on the
263 enzyme that could bind to F,Y,Q and n,I,V, respectively, consistent with the substrate recognition
264 motif shown in Fig. 4C. These data highlight the use of specificity profiling to develop optimized
265 peptide substrates that can serve as highly sensitive biochemical probes, even when compared to
266 natural peptide substrates.

267

268 **Contribution of Destructin-1 to global proteolytic activity in the *P. destructans* secretome**

269 In order to determine the contribution of Destructin-1 and related serine peptidases to
270 global proteolytic activity, we tested known protease inhibitors for inhibition of Destructin-1
271 activity. Using the IQ8 substrate, we found that the serine inhibitors PMSF, antipain, and
272 chymostatin were antagonists of Destructin-1 activity with IC₅₀ values of 46.1 μM , 85 nM, and
273 7.5 nM, respectively (Fig. 5A). Addition of the potent agonist chymostatin to *P. destructans*

274 conditioned media resulted in a 77% reduction in collagen degradation at 54 hours (Fig. 5B).
275 This confirms that Destructin-1, together with its close homologs, is the dominant collagen-
276 degrading activity secreted by *P. destructans*.

277 The contribution of the chymostatin-sensitive serine endopeptidases to the global
278 secreted proteolytic activity of *P. destructans* was evaluated using the MSP-MS assay.
279 Conditioned media was treated with either DMSO or chymostatin and incubated with the peptide
280 library. The appearance of cleavage products was assessed after 15 minutes and 1, 4 and 20
281 hours. Media that was treated with chymostatin resulted in a loss of 74% or more of the
282 cleavage sites that were detected in the DMSO control (Fig. 5C-D). This indicated that Destructin-
283 1 and its homologs are the source of most of the peptidase activity secreted from *P. destructans*.
284 Interestingly many of the cleavage sites that were resistant to chymostatin were located at the
285 amino and carboxyl terminus. In fact, treatment with the inhibitor resulted in the appearance of
286 additional cleavage sites at each termini (Fig. 5E). These sites were not detected in the control
287 assay because the 14-mer substrates were rapidly degraded into short oligopeptides by the
288 serine endopeptidases. The enzymes responsible for generation of cleavage sites at the termini
289 are likely to be the exopeptidases detected in the proteomic study (Fig. 1). Together, this data
290 indicates that chymostatin-resistant aminopeptidases and carboxypeptidases are present in the
291 conditioned media, and are revealed upon inhibition of the dominant serine endopeptidases.

292

293

294 **Discussion**

295 White-Nose Syndrome is a devastating disease that has targeted bat populations in North
296 America over the last decade. The disease is caused by *P. destructans*, a fungus that infects
297 hibernating bats and causes extensive tissue damage, particularly to the fragile membranous
298 wings (1). Connective tissue, vascular structures, and muscle fibers are degraded during

299 infection, suggesting that hydrolytic enzymes are used by the invading pathogen (25). Secreted
300 hydrolytic activities have been described by monitoring growth of *P. destructans* on a wide range
301 of *in vitro* substrates (21, 22), but the fungal proteins responsible for these activities have not
302 been elucidated.

303 In this work, we analyzed the secretome of *P. destructans*, and identified a number of
304 prevalent hydrolytic and redox enzymes. The array of secreted proteins shows similarities to
305 those described in other fungal species, including the human pathogens *C. albicans* and *A.*
306 *fumigatus* (35, 36). These fungi produce multiple hydrolytic enzymes that target host cells,
307 including peptidases that function in tissue degradation, nutrient acquisition and host invasion
308 (37). *P. destructans* secretes two serine carboxypeptidases (S10 family), an aspartyl peptidase
309 (A1 family) and three serine endopeptidases (S8 family). Our functional studies determined that
310 one or more of these peptidases degrades collagen, the major structural protein in mammalian
311 tissue (38). Therefore, we surmised that uncovering the peptidase(s) responsible for
312 degradation of this protein would be a valuable step towards understanding bat tissue invasion
313 by *P. destructans*.

314 A global and unbiased substrate profiling technology (26) was used to determine that
315 endopeptidase-type activities dominate the *P. destructans* secretome. Using a set of fluorescent
316 reporter substrates, a serine endopeptidase, Destructin-1, was identified as the principal
317 proteolytic activity present in *P. destructans* cultures. A recombinant form of the enzyme was
318 purified and shown to be capable of degrading collagen. In contrast, no cleavage was observed
319 by Destructin-1 on keratin and only very weak activity on elastin (data not shown). Collagen
320 consists of a core triple helix structure linked together by non-helical cross-links to form a
321 collagen fiber (38). Collagenases such as those produced by *Clostridium* species readily degrade
322 the helical regions of collagen (39). In contrast, however, Destructin-1 specifically cleaved the
323 non-helical cross-links between alpha 1 and 2 proteins. This disrupts the integrity of collagen

324 and may allow the fungus to penetrate further into the host tissue, possibly in combination with
325 other peptidase activities.

326 An in-depth study of recombinant Destructin-1 activity was performed using an expanded
327 MSP-MS assay containing 228 tetradecapeptides and a fluorescent library of 160,000
328 tetrapeptides. Destructin-1 was shown to readily cleave on the C-terminal side of Gln, Tyr and
329 Phe residues, particularly when hydrophobic residues were present at the P4 position and Nle,
330 Ile or Val were present at the P2 position. This study represents the most detailed substrate
331 specificity profile performed on a fungal peptidase to date, and allowed us to design a synthetic
332 peptide that was a more efficient substrate than one corresponding to the pro-Destructin-1 auto-
333 activation site.

334 The recombinant enzyme was potently inhibited by the serine peptidase antagonist
335 chymostatin, with an IC₅₀ of 7.5 nM. Treatment of *P. destructans* conditioned media with
336 chymostatin established that Destructin-1 and its close homologs were responsible for collagen
337 degradation; inhibition of these endopeptidases resulted in a loss of 85% of the peptide cleavage
338 sites in the MSP-MS assay compared to a vehicle-treated control. Interestingly, because inhibitor
339 treatment prevented the breakdown of many substrates in the MSP-MS assay, proteolytic
340 activities derived from other peptidases could now be detected. Analysis of the proteolytic
341 activities uncovered by chymostatin treatment revealed that aminopeptidases and
342 carboxypeptidases were present in the media. The potential synergy between endopeptidases
343 and exopeptidases is intriguing, as Destructin-1 may cleave intact proteins in the bat tissue,
344 resulting in the appearance of neo-termini that are then substrates for trimming by
345 exopeptidases.

346 The closest homologs of Destructin-1 are cuticle-degrading subtilisin peptidases found in
347 nematophagous fungi such as *A. conoides* and *D. varietas*. Nematophagous fungi use a variety of
348 methods to capture and kill nematodes, which are subsequently digested by the fungi (24). The

349 subtilisin-type peptidases promote penetration and digestion of nematode cuticles, and are key
350 enzymes in nematophagous species for killing of their prey (24, 29, 40-42). Interestingly, a
351 subtilisin-like serine peptidase was also recently identified in *Batrachochytrium dendrobatidis*, a
352 chytrid fungus responsible for a global decline in amphibian species. This peptidase was shown
353 to cleave anti-microbial peptides produced by frog skin, and is thus implicated in fungal survival
354 and pathogenesis (43). Furthermore, the kexin gene in *C. albicans* encodes a subtilisin-type
355 protease that is necessary for virulence due to its role in processing of proproteins (44). This
356 suggests that the family of subtilisin-type peptidases can play diverse roles as fungal virulence
357 factors.

358 In summary, this work details the composition of the *P. destructans* secretome and
359 identifies the serine peptidase Destructin-1 as the major extracellular, collagen-degrading
360 endopeptidase. Future studies will further address the potential role of Destructin-1 and its
361 homologs as novel virulence factors, and will determine the role of other secreted proteins in
362 promoting infection of epithelial tissues. It is expected that a combination of hydrolytic activities
363 are used by *P. destructans* to invade and destroy bat tissues. As such, limiting these hydrolytic
364 activities is predicted to be a successful approach for the prevention or treatment of WNS in bats.

365

366 **Materials and Methods**

367 Proteome analysis, biochemical assays, protein expression and protein purification were
368 performed as described in *SI Materials and Methods*.

369

370 **Acknowledgements**

371 This research was funded in part by the UCSF Program for Breakthrough Biomedical Research,
372 and by the Sandler Foundation (to C.S.C.). Mass spectrometry analysis was performed in the Bio-
373 Organic Biomedical Mass Spectrometry Resource at UCSF (A.L. Burlingame, Director) supported

374 by the Biomedical Technology Research Centers program of the NIH National Institute of General
375 Medical Sciences, NIH NIGMS 8P41GM103481. Work was also supported by the NIH
376 T32GM007601 (to C.B.) and P50GM082250 (to C.S.C). The authors also thank Jeremy A. Horst
377 for structural modeling assistance with the Destructin-1 homology model.

378

379 **References**

- 380 1. Blehert DS (2012) Fungal disease and the developing story of bat white-nose syndrome.
381 *PLoS Pathog* 8(7):e1002779.
- 382 2. Blehert DS, *et al.* (2009) Bat white-nose syndrome: an emerging fungal pathogen? *Science*
383 323(5911):227.
- 384 3. Coleman J & Hibbard C (2013) News Release. *U.S. Fish and Wildlife*
385 ([http://batcon.org/pdfs/whitenose/2013 WNS grants to states final.pdf](http://batcon.org/pdfs/whitenose/2013_WNS_grants_to_states_final.pdf)).
- 386 4. Frick WF, *et al.* (2010) An emerging disease causes regional population collapse of a
387 common North American bat species. *Science* 329(5992):679-682.
- 388 5. Boyles JG, Cryan PM, McCracken GF, & Kunz TH (2012) Economic Importance of Bats in
389 Agriculture. *Science* 332:41-42.
- 390 6. Minnis AM & Lindner DL (2013) Phylogenetic evaluation of *Geomyces* and allies reveals no
391 close relatives of *Pseudogymnoascus destructans*, comb. nov., in bat hibernacula of eastern
392 North America. *Fungal Biol* 117(9):638-649.
- 393 7. Lorch JM, *et al.* (2011) Experimental infection of bats with *Geomyces destructans* causes
394 white-nose syndrome. *Nature* 480(7377):376-378.
- 395 8. Verant ML, Boyles JG, Waldrep W, Jr., Wibbelt G, & Blehert DS (2012) Temperature-
396 dependent growth of *Geomyces destructans*, the fungus that causes bat white-nose
397 syndrome. *PLoS One* 7(9):e46280.
- 398 9. Warnecke L, *et al.* (2012) Inoculation of bats with European *Geomyces destructans*
399 supports the novel pathogen hypothesis for the origin of white-nose syndrome. *Proc Natl*
400 *Acad Sci U S A* 109(18):6999-7003.
- 401 10. Meteyer CU, *et al.* (2009) Histopathologic criteria to confirm white-nose syndrome in bats.
402 *Journal of veterinary diagnostic investigation : official publication of the American*
403 *Association of Veterinary Laboratory Diagnosticians, Inc* 21(4):411-414.

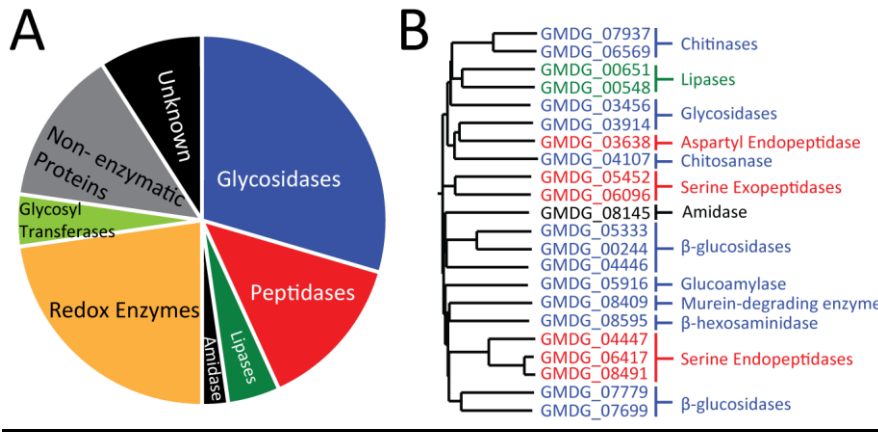
- 404 11. Wibbelt G, *et al.* (2013) Skin lesions in European hibernating bats associated with
405 *Geomyces destructans*, the etiologic agent of white-nose syndrome. *PLoS One* 8(9):e74105.
- 406 12. Puechmaille SJ, *et al.* (2013) Pan-European Distribution of White-Nose Syndrome Fungus
407 (*Geomyces destructans*) Not Associated with Mass Mortality. *PLoS One* 6:e19167.
- 408 13. Zukan J, *et al.* (2014) White-nose syndrome fungus: a generalist pathogen of hibernating
409 bats. *PLoS One* 9(5):e97224.
- 410 14. Yike I (2011) Fungal proteases and their pathophysiological effects. *Mycopathologia*
411 171(5):299-323.
- 412 15. Monod M, *et al.* (2002) Secreted proteases from pathogenic fungi. *International journal of*
413 *medical microbiology : IJMM* 292(5-6):405-419.
- 414 16. Naglik J, Albrecht A, Bader O, & Hube B (2004) *Candida albicans* proteinases and
415 host/pathogen interactions. *Cell Microbiol* 6(10):915-926.
- 416 17. Baldo A, *et al.* (2012) Mechanisms of skin adherence and invasion by dermatophytes.
417 *Mycoses* 55(3):218-223.
- 418 18. Achterman RR & White TC (2012) Dermatophyte virulence factors: identifying and
419 analyzing genes that may contribute to chronic or acute skin infections. *International*
420 *journal of microbiology* 2012:358305.
- 421 19. Santos AL & Braga-Silva LA (2013) Aspartic protease inhibitors: effective drugs against
422 the human fungal pathogen *Candida albicans*. *Mini reviews in medicinal chemistry*
423 13(1):155-162.
- 424 20. Park M, Do E, & Jung WH (2013) Lipolytic enzymes involved in the virulence of human
425 pathogenic fungi. *Mycobiology* 41(2):67-72.
- 426 21. Chaturvedi V, *et al.* (2010) Morphological and molecular characterizations of
427 psychrophilic fungus *Geomyces destructans* from New York bats with White Nose
428 Syndrome (WNS). *PLoS One* 5(5):e10783.

- 429 22. Reynolds HT & Barton HA (2014) Comparison of the white-nose syndrome agent
430 *Pseudogymnoascus destructans* to cave-dwelling relatives suggests reduced saprotrophic
431 enzyme activity. *PLoS One* 9(1):e86437.
- 432 23. Monod M & Borg-von ZM (2002) Secreted aspartic proteases as virulence factors of
433 *Candida* species. *Biological chemistry* 383(7-8):1087-1093.
- 434 24. Yang J, Tian B, Liang L, & Zhang KQ (2007) Extracellular enzymes and the pathogenesis of
435 nematophagous fungi. *Applied microbiology and biotechnology* 75(1):21-31.
- 436 25. Cryan PM, Meteyer CU, Boyles JG, & Blehert DS (2010) Wing pathology of white-nose
437 syndrome in bats suggests life-threatening disruption of physiology. *BMC Biol* 8:135.
- 438 26. O'Donoghue AJ, *et al.* (2012) Global identification of peptidase specificity by multiplex
439 substrate profiling. *Nature methods* 9(11):1095-1100.
- 440 27. Colaert N, Helsens K, Martens L, Vandekerckhove J, & Gevaert K (2009) Improved
441 visualization of protein consensus sequences by iceLogo. *Nature methods* 6(11):786-787.
- 442 28. Yang J, *et al.* (2007) Cloning and characterization of an extracellular serine protease from
443 the nematode-trapping fungus *Arthrobotrys conoides*. *Archives of microbiology*
444 188(2):167-174.
- 445 29. Yang J, *et al.* (2007) Purification and cloning of a novel serine protease from the
446 nematode-trapping fungus *Dactylellina varietas* and its potential roles in infection against
447 nematodes. *Applied microbiology and biotechnology* 75(3):557-565.
- 448 30. Page MJ & Di Cera E (2008) Serine peptidases: classification, structure and function. *Cell*
449 *Mol Life Sci* 65(7-8):1220-1236.
- 450 31. Petersen TN, Brunak S, von Heijne G, & Nielsen H (2011) SignalP 4.0: discriminating signal
451 peptides from transmembrane regions. *Nature methods* 8(10):785-786.
- 452 32. Harris JL, *et al.* (2000) Rapid and general profiling of protease specificity by using
453 combinatorial fluorogenic substrate libraries. *Proc Natl Acad Sci U S A* 97(14):7754-7759.

- 454 33. O'Donoghue AJ, *et al.* (2008) Inhibition of a secreted glutamic peptidase prevents growth
455 of the fungus *Talaromyces emersonii*. *J Biol Chem* 283(43):29186-29195.
- 456 34. Small JL, *et al.* (2013) Substrate specificity of MarP, a periplasmic protease required for
457 resistance to acid and oxidative stress in *Mycobacterium tuberculosis*. *J Biol Chem*
458 288(18):12489-12499.
- 459 35. Sorgo AG, *et al.* (2010) Mass spectrometric analysis of the secretome of *Candida albicans*.
460 *Yeast* 27(8):661-672.
- 461 36. Wartenberg D, *et al.* (2011) Secretome analysis of *Aspergillus fumigatus* reveals Asp-
462 hemolysin as a major secreted protein. *International journal of medical microbiology :*
463 *IJMM* 301(7):602-611.
- 464 37. Schaller M, Borelli C, Korting HC, & Hube B (2005) Hydrolytic enzymes as virulence
465 factors of *Candida albicans*. *Mycoses* 48(6):365-377.
- 466 38. Shoulders MD & Raines RT (2009) Collagen structure and stability. *Annu Rev Biochem*
467 78:929-958.
- 468 39. Eckhard U, Huesgen PF, Brandstetter H, & Overall CM (2014) Proteomic protease
469 specificity profiling of clostridial collagenases reveals their intrinsic nature as dedicated
470 degraders of collagen. *Journal of proteomics* 100:102-114.
- 471 40. Tunlid A, Rosen S, Ek B, & Rask L (1994) Purification and characterization of an
472 extracellular serine protease from the nematode-trapping fungus *Arthrobotrys oligospora*.
473 *Microbiology* 140 (Pt 7):1687-1695.
- 474 41. Li J, *et al.* (2010) New insights into the evolution of subtilisin-like serine protease genes in
475 *Pezizomycotina*. *BMC Evol Biol* 10:68.
- 476 42. Huang X, Zhao N, & Zhang K (2004) Extracellular enzymes serving as virulence factors in
477 nematophagous fungi involved in infection of the host. *Res Microbiol* 155(10):811-816.

- 478 43. Thekkiniath JC, Zabet-Moghaddam M, San Francisco SK, & San Francisco MJ (2013) A
479 novel subtilisin-like serine protease of *Batrachochytrium dendrobatidis* is induced by
480 thyroid hormone and degrades antimicrobial peptides. *Fungal Biol* 117(6):451-461.
- 481 44. Newport G, *et al.* (2003) Inactivation of Kex2p diminishes the virulence of *Candida*
482 *albicans*. *J Biol Chem* 278:1713-1720.
- 483

484 **Figure Legends**



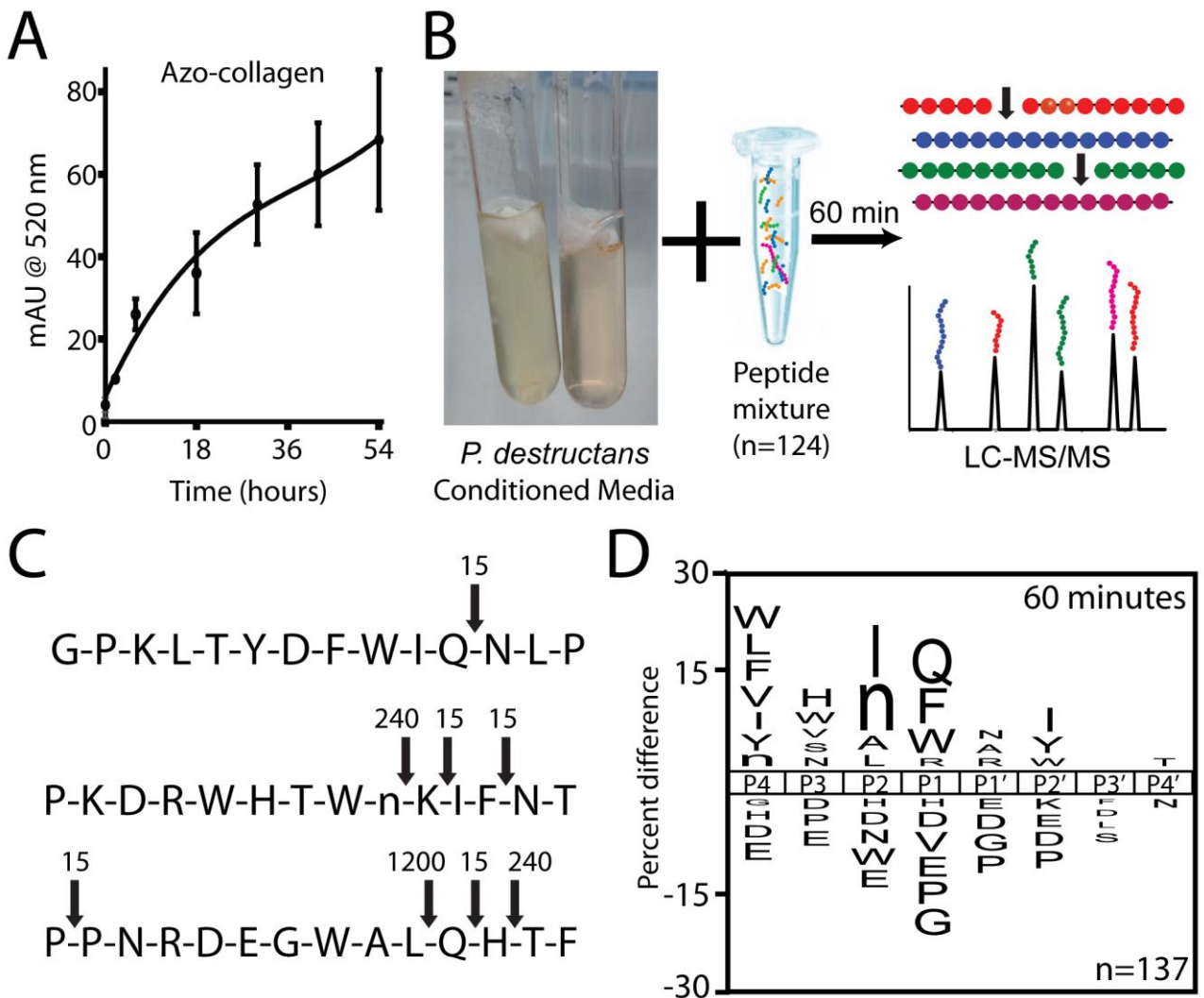
485

486 **Figure 1.** Analysis of the secretome of *P. destructans*.

487 (A) Composition of enzymatic activities present in conditioned medium from *P. destructans*. (B)

488 Phylogenetic relationship between hydrolytic activities secreted by *P. destructans*. Note that

489 secreted activities include three families of peptidases.



490

491 **Figure 2. Peptidase substrate specificity from *P. destructans* conditioned medium.**

492 (A) Cleavage of azo-collagen by conditioned medium from *P. destructans*. (B) Outline of the MSP-

493 MS assay used to examine peptidase activities in the secretome of *P. destructans*. Conditioned

494 media was incubated with a mixture of 124 peptides and sampled at subsequent time points by

495 LC-MS/MS peptide sequencing. (C) Cleavage sites are shown for three representative peptides in

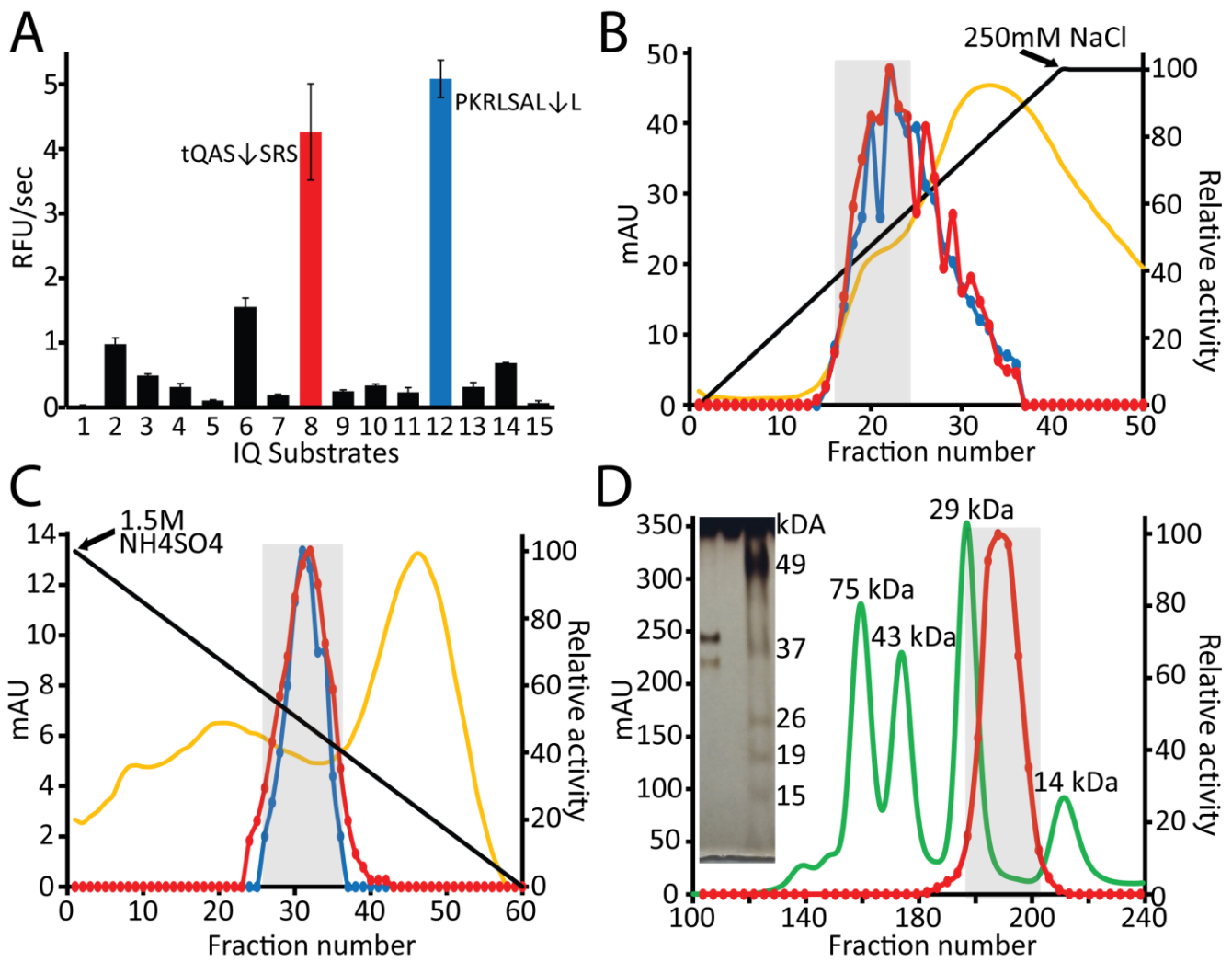
496 the MSP-MS assay. Incubation time at which cleavage events were first observed is indicated in

497 minutes. (D) iceLogo generated from the pattern of cleavage events at 60 min shows the

498 specificity of peptidase activity. Amino acids that are most frequently observed at each position

499 are shown above the axis, and amino acids least frequently observed are shown below the axis.

500

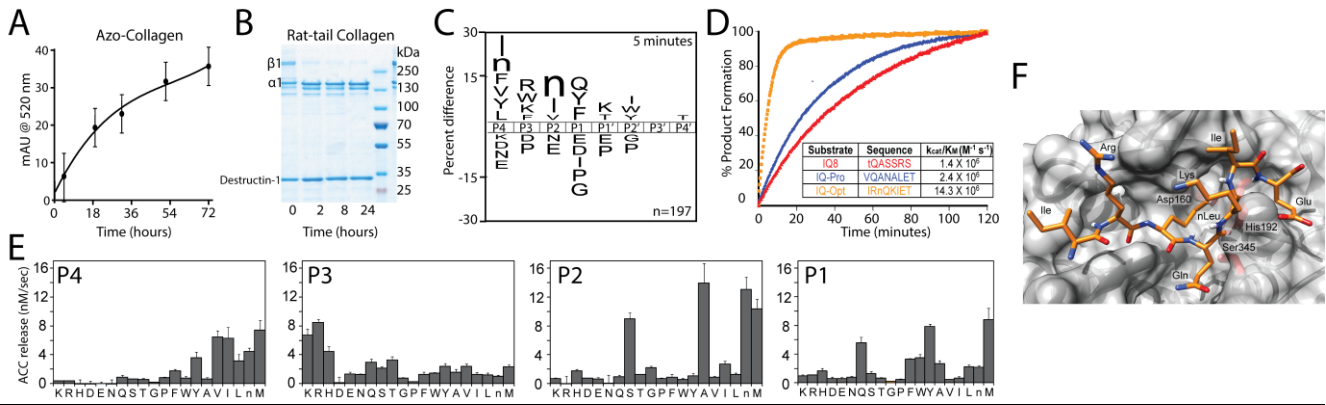


501

502 **Figure 3. Purification of a serine S8 peptidase, Destructin-1, from *P. destructans***
 503 **conditioned medium.**

504 (A) Analysis of relative cleavage rates by *P. destructans* conditioned media on 15 different IQ
 505 substrates. Conditioned medium was purified using a 3-step process using (B) DEAE sepharose,
 506 (C) Phenyl sepharose, and (D) gel filtration. Peptidase activity was monitored using cleavage of
 507 IQ8 (red line) and IQ12 (blue line) substrates. Yellow line indicates total protein by absorbance
 508 at 280 nm and the grey box shows the fractions that were pooled for subsequent separation or
 509 characterization. Green line indicates protein standards on gel filtration column. The most
 510 purified fraction was also analyzed on a silver-stained SDS-PAGE gel (inset, part D).

511



512

513 **Figure 4. Characterization of recombinant Destructin-1 activity.**

514 (A) Destructin-1 was co-incubated with Azo-collagen for 54 hours at 20°C and the release of Azo

515 dye measured photometrically at 520 nm. (B) Cleavage and analysis of collagen degradation by

516 Destructin-1 by SDS-PAGE. α 1 and β 1 bands indicate the major protein components of collagen.

517 (C) iceLogo analysis of the recombinant Destructin-1 protein in the MSP-MS assay. (D)

518 Comparison of kinetics of cleavage between IQ8, IQ-Pro and IQ-Opt substrates. k_{cat}/K_m values

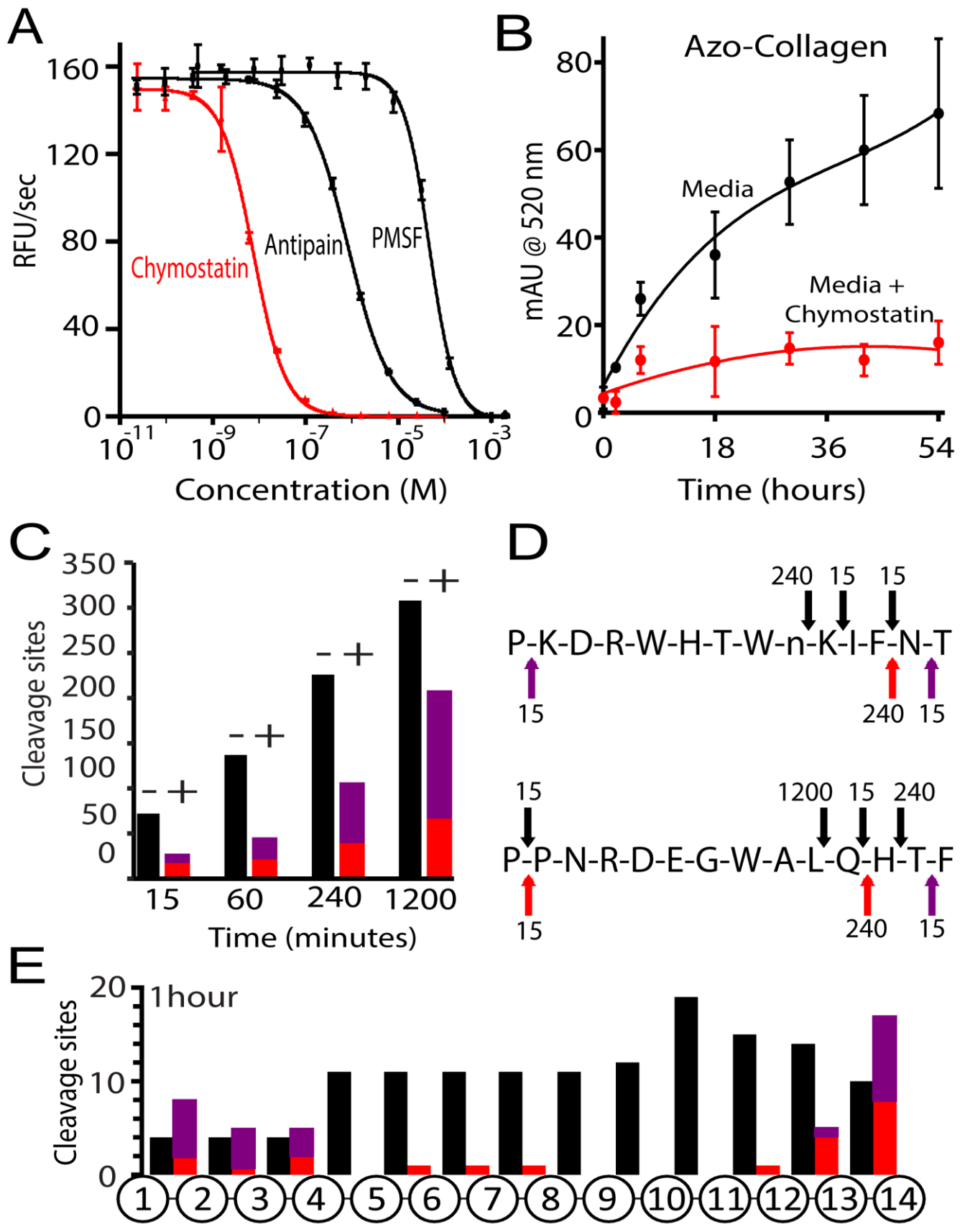
519 are shown for each IQ substrate. (E) PS-SCL profiling of the recombinant Destructin-1 protein to

520 determine cleavage specificity at P1-P4 positions. (F) Homology model of the Destructin-1

521 substrate-binding pocket (grey ribbons and semitransparent surface) with the IQ-Opt sequence

522 IRnQKIE shown in orange, and the catalytic triad residues Asp160, His192, and Ser345 in red.

523



525 **Figure 5. Inhibition of Destructin-1 reveals the presence of other peptidases in the *P.***
526 ***destructans* secretome.**

527 **(A)** Inhibition of Destructin-1 peptidase activity using chymostatin, antipain or PMSF inhibitors.
528 Activity assays were performed using the IQ8 substrate. **(B)** Cleavage of azo-collagen by
529 Destructin-1 in the presence or absence of chymostatin. **(C)** Total number of Destructin-1
530 cleavage sites in the MSP-MS assay in the presence (red) or absence (black) of chymostatin.
531 Cleavage sites that are only present in the presence of chymostatin are colored purple. **(D)**
532 Examples of two peptides from the MSP-MS assay cleaved by recombinant Destructin-1 in the
533 presence (red/purple arrows) or absence (black arrows) of chymostatin. The time in minutes at
534 which cleavage events were first detected is indicated. **(E)** Positional analysis of peptide
535 cleavage by Destructin-1 after 1 hour incubation in the MSP-MS assay in the presence or absence
536 of chymostatin. Color scheme is the same as in D.

537